Evaluating the Synergy of Relative and Absolute Indoor Localization in Industrial Spaces

Fabian Hölzke, Hannes Raddatz, Frank Golatowski, Dirk Timmermann

Institute of Applied Microelectronics and CE
University of Rostock,
Rostock, Germany
Email: fabian.hoelzke2@uni-rostock.de

Julian Lategahn

Comnovo GmbH
Dortmund, Germany
Email: lategahn@comnovo.de

***Abstract*—Industrial Internet of Things (IIoT) applications benefit from the knowledge of the device and user positions in a manifold way. Reliable indoor navigation combined with IIoT enables Location-Based-Services (LBS) such as assistance functions of moveable actuators. A crane which follows its operator can significantly increase the efficiency of the process. Safety mechanisms are also enhanced by positioning information. For example, exclusion areas where only automated devices are operating can be implemented. In this paper a novel localization framework is introduced to fuse sensor data from either absolute or relative positioning sources. The core of the framework is an Extended Kalman-Filter (EKF) architecture that is able to handle data from several different sources. Each localization source needs to fulfill requirements regarding data representation and structure defined by the framework, e.g., current state and variance. The approach is verified in a real world scenario with two different sensor types as information sources: Ultra Wide Band localization and Pedestrian Dead Reckoning. We show that the combination of these technologies improves the localization accuracy and evaluate advantages and drawbacks of this approach.**

I. Introduction

Localization in industrial spaces plays an increasingly important role in the context of new assistance and safety functions of autonomous machines. The German initiative *Industrie 4.0*, among other things, aims to enhance traditional industries by interconnecting devices with modern communication protocols to enable Machine-to-Machine (M2M) communication, increase productivity and safety as well as support the development of novel approaches for manufacturing and material handling. Localization of workers and mobile machinery plays a crucial role to enable a machine to provide assistance, autonomous and safety functions.

For example, cranes or forklifts may route autonomously to a given target position and reroute dynamically based on changes in the environment. However, autonomous machines are prone to accidents with other mobile machinery and especially humans. To prevent collisions and to enable assistance functions, a reliable and accurate localization is crucial.

Common infrastructure based localization approaches have limited accuracy and are prone to disturbance (Bluetooth, WiFi fingerprinting). Relative localization such as dead reckoning based methods are comparably inexpensive but exhibit degrading accuracy over time. We present a localization framework that utilizes sources of both, relative and absolute, positioning data to enable reliable and accurate indoor positioning in industrial spaces. We demonstrate this approach using Pedestrian Dead Reckoning (PDR) as a relative and Ultra-Wide Band (UWB) as a absolute positioning technology. This approach is not limited to humans. Machines such as cranes and forklifts commonly provide data on the current speed or odometry, which are leveraged as a source of relative positioning. This paper highlights advantages and drawbacks of both positioning approaches and how a combination improves the positioning accuracy and mitigates these drawbacks. Additionally, the described architecture is not limited to specific localization technologies. It supports generic sources of absolute positions and relative displacement.

This paper is structured as follows: Section II describes related work regarding UWB and PDR based positioning and the combination of both approaches. The architecture to combine multiple localization sources is presented in Section III. The localization methods we use are described in Section IV, with the emphasis in Section IV-A on UWB and in Section IV-B on PDR, and in Section V on the the fusion of both methods. We conducted experiments to verify our methods as described in Section VI. The experimental results are presented in Section VII. Final conclusions are drawn in Section VIII.

II. Related Work

Radio based localization is popular in the field of industrial automation. Especially UWB is used in such environments due to the high positioning accuracy compared to WiFi and Bluetooth. In [1] a localization algorithm for industrial environments is presented, while in [2] the connectivity of UWB devices in such environments is tested. The authors of [3] compare three types UWB systems with regards to accuracy and precision. WiFi and Bluetooth based approaches offer low cost and the infrastructure is often already available. The authors in [4] evaluate Bluetooth while in [5] a WiFi fingerprinting approach is used.

Pedestrian Dead Reckoning (PDR) uses wearable inertial sensors to compute single steps and their direction. The users' relative displacement is computed as the sum of the taken

steps [6]. A comparably precise method of step detection is using Zero-Velocity-Updates (ZUPT) with foot mounted sensors. Here, the acceleration of the foot is integrated twice to compute the displacement caused by one step. The following zero-velocity period of contact to the ground is used to evaluate errors in the estimated velocity from the first integration and to subsequently correct the step length estimation [7].

An alternative to directly measuring a single step is to recognize whether or not a step has been performed and then estimate the stride length [8]. For this, the measured acceleration of a hand-held or wearable sensor is analyzed for exceeded thresholds, peaks, periodic patterns or a combination of these methods. Gyroscopic data is used to recognize the swing of arms or legs [9], [10]. Machine learning techniques are employed to further improve the step detection reliability [11], [12].

The quality of positioning with dead reckoning degrades over time as errors in step length and orientation as well as step count accumulate. A challenge of radio based localization is the introduction of ranging errors when line of sight to a base station is lost. To reduce the need of ranging error mitigation and to limit the increasing error of dead reckoning, relative and absolute positioning approaches like PDR and UWB can be combined [13], [14]. The authors of [15] fuse step detection and step length estimation with low frequency UWB updates to limit the PDR location drift using an Unscented Kalman-Filter. Another approach is presented in [16], where inertial sensor data is combined with UWB positioning using an Extended Kalman-Filter (EKF).

The authors of [17] show that a magnetometer that is used to establish a fixed reference frame for the orientation of PDR requires sophisticated correction methods and the presence of a building map in industrial spaces. Disturbances due to ferromagnetic materials and heavy electric machinery degrade the compass measurement.

III. Architecture

The general pattern of our localization approach is the combination of relative and absolute positioning data. Relative positioning technologies provide the displacement relative to a known previous position. A drawback of relative positioning is an increasing positioning error through accumulated measurement errors. Because of this, absolute positioning data is used to limit the error growth. The localization of humans is realized through the relative positioning with PDR and absolute positioning using UWB. Machines are localized using the relative odometry data of their drives and absolute UWB information. We combine pre-processed estimates of the absolute position or position change based on the raw sensor data. Consequently, the fusion approach is loosely coupled and independent from the exact type of raw sensor data, e.g. instead of distance measurements from UWB, we feed the position estimate to the fusion process.

A device-level view is seen in Fig. 1. We are proposing a device with deterministic computing capability. All incoming pre-processed data is fed to a real-time software component that fuses the data to derive a position estimate. This estimate is used by other system components for movement control tasks of the localized device, e.g. a crane, and also published via an Industrial Internet of Things (IIoT) component to the industrial network to enable advanced control and safety features.

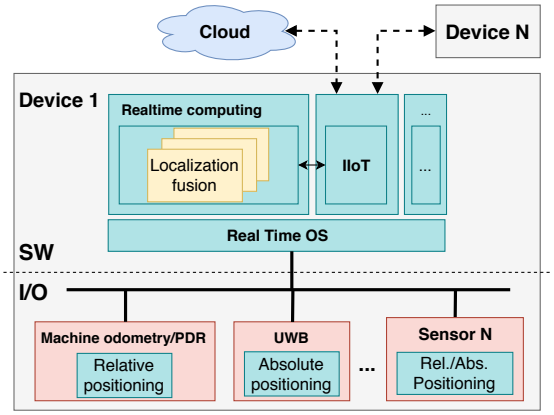

Figure 1: Device architecture showing the interconnection of various localization data sources, the processing in a real-time software component and distribution of localization via IIoT.

IV. Localization

In the following subsections, we are presenting the UWB positioning scheme using an EKF and the processing of inertial sensor data to achieve PDR.

A. Absolute Positioning using UWB

We use an UWB system as an example for absolute positioning for mobile actors, processed by an EKF. The initial position is computed by a simple trilateration least squares algorithm. The state transition function is assumed to be the linear constant velocity model, so it is as follows:

$$\begin{pmatrix} p_{x,k} \\ p_{y,k} \\ v_{x,k} \\ v_{y,k} \end{pmatrix} = \begin{pmatrix} 1 & 0 & d_t & 0 \\ 0 & 1 & 0 & d_t \\ 0 & 0 & 1 & 0 \\ 0 & 0 & 0 & 1 \end{pmatrix} \begin{pmatrix} p_{x,k-1} \\ p_{y,k-1} \\ v_{x,k-1} \\ v_{y,k-1} \end{pmatrix} \quad (1)$$

Since the noise of the system $\boldsymbol{\omega}_k$ is only related to the constant update rate of the system, the covariance Q is also assumed to be constant.

The measurement model is based on the euclidean distance:

$$d^a = \sqrt{(x_k - x^a)^2 + (y_k - y^a)^2 + (h_k - h^a)^2} + \boldsymbol{v}_k \quad (2)$$

x_k, y_k, h_k denote the coordinates of the tag and x^a, y^a, h^a the coordinates at the a^{th} anchor. The height of the tag h^k and the anchors h^a is assumed to be constant. Once again the noise of the measurement model $\boldsymbol{v}_k$ is constant.

B. Relative Positioning using PDR

We employ PDR as a source of relative positioning, using tri-axial acceleration and angular-rate measurements of an inertial measurement unit (IMU) attached to the top of one foot of the user.

The orientation of the sensor relative to the global frame of reference is computed using a Magdwick filter with acceleration and angular rate as inputs. We use the resulting unit quaternion to match and subtract the global gravity vector and to compute the acceleration of the sensor without the influence of gravity. In contrast to the original description of the filter in [18], we do not employ a magnetometer. Consequently, we track the change of heading, but do not calibrate to the absolute real world heading for PDR.

The sensor placement on the foot allows for the distinction of stand and swing phases of the foot during each stride. A stand phase of the foot is defined as the period of ground contact in which the expected velocity of the sensor is zero. It is detected by the computation of the signal energy of both angular rate (Eq. (3)) and acceleration (Eq. (4)) in a window of N samples around sensor sample k with the magnitude of the three-dimensional vectors of acceleration a and angular rate ω, as well as the gravity constant g. A stand phase is recognized if both signal energies are below the respective thresholds th_a and th_ω as described by Eq. (5). Otherwise, a swing phase is detected.

$$E_\omega^k = \frac{1}{N} \sum_{i=k-\frac{N}{2}}^{k+\frac{N}{2}} |\omega_i|^2 \tag{3}$$

$$E_a^k = \frac{1}{N} \sum_{i=k-\frac{N}{2}}^{k+\frac{N}{2}} (|a_i| - g)^2 \tag{4}$$

$$stand = E_a < th_a \wedge E_\omega < th_\omega \tag{5}$$

During the swing phase, the current acceleration sample is first aligned to the global reference frame. Secondly, gravity is subtracted from the vertical axis. Finally, the current velocity v_k is computed by integrating the transformed acceleration as described by Eq. (6) with sample k and sampling time interval T.

$$v_k = v_{k-1} + a_k T \tag{6}$$

The following stand phase signals the end of the step and we employ ZUPT for the correction of velocity drift as described in [19]. The corrected velocity v'_k is summed over the number of samples of the swing phase M_{sw} as described by Eq. (7). The resulting displacement s is the current step vector used for PDR.

$$s = \sum_{k=0}^{M_{sw}-1} v'_k T \tag{7}$$

The start of the next swing phase is used to finally compute the pedestrians current velocity v as described by Eq. (8), with M_{st} as the count of samples in the finished stand phase. The orientation change $\Delta\Theta$ is computed as the difference of orientation from beginning to end of one step.

$$v = \frac{|s|}{(M_{sw} + M_{st})T} \tag{8}$$

V. Fusion of Absolute and Relative Localization

The loosely coupled fusion concept is based on a previous work [20]. Regarding measurement updates with relative positioning data, the idea is that estimating a velocity vector is more stable than estimating the heading directly. Furthermore, since no absolute heading is available, it is also advantageous to estimate it from the velocity vector.

If not stated otherwise, the process of the fusion EKF is propagated as follows:

$$\tilde{x}_k = \begin{pmatrix} p_{x,k} \\ p_{y,k} \\ v_{x,k} \\ v_{y,k} \end{pmatrix} = \begin{pmatrix} 1 & 0 & dt & 0 \\ 0 & 1 & 0 & dt \\ 0 & 0 & 1 & 0 \\ 0 & 0 & 0 & 1 \end{pmatrix} \begin{pmatrix} p_{x,k-1} \\ p_{y,k-1} \\ v_{x,k-1} \\ v_{y,k-1} \end{pmatrix} \tag{9}$$

with fused positing p_k and velocity v_k at current time instance k.

There are movable actors of different kinds in an industrial environment like cranes, forklifts and humans. From a localization perspective it is possible to divide them into two groups. The first group contains devices that are restricted to movement on rails that can directly measure their movement direction, while members of the other group, e.g. forklifts and humans, are able to measure their velocity v and the orientation change $\Delta\Theta$.

Based on the different approaches, the state updates are described in the following, with emphasis in subsection V-A on orientation change and velocity measurements and in V-B on absolute position measurements.

The position update with a directly measured movement vector is straight forward. The velocity measurement in each direction $v_{x,k}$ and $v_{y,k}$ is propagated to the filter as a measurement. With a one to one relation to the velocity state. The covariance of the velocity $\boldsymbol{R}^v$ is assumed to be constant.

A. Velocity and Orientation Change Measurements

Actors with orientation updates that are more frequent than the absolute positioning updates use the state prediction update described in [20] instead of Eq. 9. We employ a modified version of this approach for the the PDR system described in Section IV-B with low frequency orientation updates. The architecture outlined in this chapter is visualized in Fig. 2

The rotation change $\Delta\Theta$ is propagated to the process update of a separate PDR-EKF to compute the PDR state prediction $\tilde{x}_k^{pdr}$ with v_{k-n} and p_{k-n} as the velocity and position state at the last orientation update $\hat{x}_{k-n}$ of the fusion EKF:

$$\begin{pmatrix} p_{x,k} \\ p_{y,k} \\ v_{x,k} \\ v_{y,k} \end{pmatrix} = \begin{pmatrix} p_{x,k-n} + v_{x,k} dt + \epsilon_x \\ p_{y,k-n} + v_{y,k} dt + \epsilon_y \\ v_{x,k-n} \cos(\Delta\Theta + \epsilon_\Theta) - v_{y,k-n} \sin(\Delta\Theta + \epsilon_\Theta) \\ v_{y,k-n} \sin(\Delta\Theta + \epsilon_\Theta) + v_{x,k-n} \cos(\Delta\Theta + \epsilon_\Theta)) \end{pmatrix} \tag{10}$$

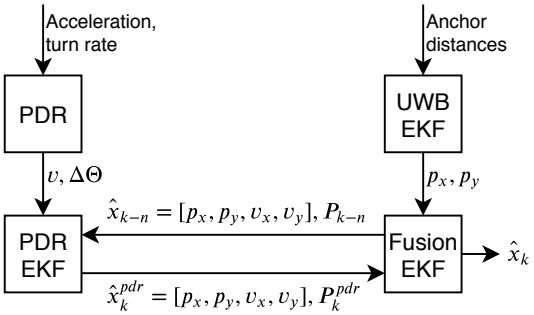

Figure 2: The flow from raw sensor data to a fused position and velocity estimate $\hat{x}_k$ with PDR and UWB as exemplary sensor inputs.

The process covariance estimate P_k^{pdr} is propagated using the appropriate Jacobi matrices of Eq. (10) and the process covariance matrix P_{k-n} at the last orientation update of the fusion EKF.

If the actor is moving straight, i.e. $\Delta\Theta < a$ with a as a threshold value, a velocity measurement update is applied with the measurement $\boldsymbol{z}_k^v$ as described in Eq. (11) to compute the state estimate $\hat{x}_k^{pdr}$.

$$\boldsymbol{z}_k^v = \sqrt{v_{x,k}^2 + v_{y,k}^2} + \boldsymbol{\nu}_k^v \tag{11}$$

If the update is applied to a state prediction with large $\Delta\Theta$, the velocity state tends to have a large orientation error. This is due to an unbalanced, albeit correct, error covariance prediction, of the two velocity axes of $\tilde{x}_k^{pdr}$. If the velocity measurement update is not applied we set $\hat{x}_k^{pdr} = \tilde{x}_k^{pdr}$.

$\hat{x}_k^{pdr}$ is fed back to the fusion EKF and handled as a measurement with

$$\boldsymbol{H}^{pdr} = I_{4\times4}. \tag{12}$$

The diagonal of P_k^{pdr} is used as the measurement covariance matrix for the final measurement update of the fusion EKF. Additionally, the covariance matrix of the fusion EKF and the absolute position measurements are supplemented with a penalty that decreases over time. This way, the PDR update gains more weight in the short term and variations by absolute positioning are compensated. On the other hand, the PDR-EKF still converges towards the absolute measurements and the drift inherent to relative positioning is compensated.

B. Location Update with Absolute Localization

The absolute position information is propagated as a measurement to the EKF and independent from the relative position information. If the position is not calculated in the same coordinate system as the fusion, the rotation and translation must be known and transformed before propagating it to the EKF. The measurement vector $z_k^{(n)}$ of sensor n consists only of the position information:

$$\boldsymbol{z}_k^{(n)} = \begin{pmatrix} p_{x,k}^{(n)} \\ p_{y,k}^{(n)} \end{pmatrix} \tag{13}$$

with

$$\boldsymbol{H}^p = \begin{pmatrix} 1 & 0 & 0 & 0 \\ 0 & 1 & 0 & 0 \end{pmatrix}. \tag{14}$$

Each sensor which is providing an absolute position is assumed to be independent with a known covariance matrix $\boldsymbol{R}_k^{(n)}$. The update rate of a sensor must not be specified.

VI. Experimental setup

We verify the proposed fusion method for pedestrians on several test tracks in a lecture hall of the Institute of Applied Microelectronics and CE. The aim is to verify the complementary properties of UWB and PDR, especially concerning the estimation of movement direction and its impact on positioning accuracy. The employed IMU on the users' foot is a Hillcrest FSM-9 with a sampling rate of 125 Hz. The UWB system is based on the Decawave DWM 1000 chipset, producing ranging measurements at a frequency of 4 Hz. The corresponding EKF updates the position estimate with the same frequency.

The first experiment covers multiple tracks with a length of approximately 10 m. One track consists of walking straight, while the others contain one change of direction with a turn angle ranging from $45°$ to $180°$ in $45°$ increments. A $90°$ turn is examined with turn radii of 0 m (i.e. immediate turn), 1.05 m, 1.85 m and 2.63 m. Each track was walked five times in each direction. The main interest of the first experiment lies in the behavior of orientation estimation of both positioning technologies. Consequently, each track is traversed with an UWB receiver tag placed above the head of the user, emulating the placement on a helmet. This reduces ranging errors caused by shadowing of the users body and results in fewer errors in the orientation estimate of UWB. The direction of the UWB-EKF velocity estimate is used as the orientation estimate of UWB. The UWB anchor placement and ground truth of the tracks is shown in Fig. 3.

In order to compare the characteristics of the orientation estimation, we compare the timing of start and end of turn indication of both technologies. Typically, Kalman-filtered estimates take some time to converge to a new steady state, i.e. a new orientation. If PDR provides a faster estimate, an improvement in the accuracy of the fused position is expected.

The second experiment tests the actual accuracy of our fusion method and introduces non-line-of-sight (NLOS) errors to UWB. It covers two tracks: walking straight and making an immediate $90°$ turn. The UWB receiver tag is placed on the shoulder of the test person. We introduce a ferromagnetic obstacle to the side of the track. This object is positioned at 0.8 m height from the ground with a total height and a width of 2.03 m. It is positioned 0.8 m to the left and half way down of the straight track. The placement for the $90°$ turn is shown in Fig. 5. The object simulates view obstructions such as loads on a crane in an industrial environment. We compare the results of these two tests with the fused location from the same tracks under ideal circumstances as described in experiment one. Again, each track was walked five times in each direction.

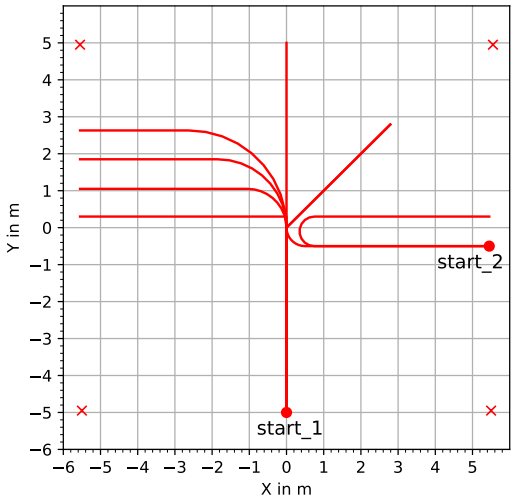

Figure 3: Ground truth of the pedestrian tracks with various turn angles. Straight tracks and tracks with turns of 45° and 90° begin at *start_1*. Tracks with 135° and 180° turns begin at *start_2*. UWB anchor placements are marked as red crosses.

VII. Experimental Results

The difference in timing of orientation change indication for PDR and UWB-EKF is presented in Tab. I. We evaluate the time difference when a significant change of direction is beginning and ending according to PDR and UWB. This shows inherent differences of PDR and UWB that are exploited in our fusion approach. We define the start and end of a turn when the measurements show a deviation of 11.5° from the initial or final orientation respectively. This tolerance band compensates noisy UWB measurements and drift of PDR. Fig. 4 shows these points in time for one characteristic recording of a immediate 90° turn.

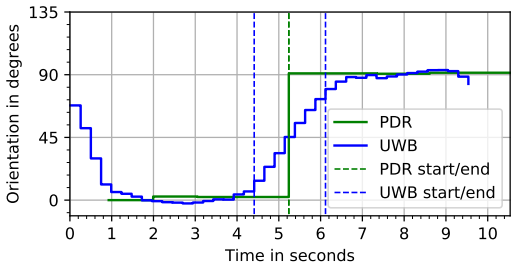

Figure 4: Orientation over time at an immediate 90° turn.

The measurements show that PDR indicates the beginning of a turn later than UWB. However, UWB takes longer than PDR to indicate the final orientation. The initial delay of PDR is most pronounced at the immediate 90°_0 and 45°_0 turns, and almost immediate 135° turn with a difference of about 0.5 seconds to UWB. This delay almost vanishes on tracks with a gradual change of orientation like the other 90° turns and the 180° turn. There is no clear influence of turn angle on the time of first orientation change. When approaching the final orientation, PDR is on average 0.56 seconds faster than UWB, also showing no clear correlation with turn radius or turn angle.

TABLE I: Difference of timing for start and end of turn indication by PDR and UWB in seconds. A positive value indicates PDR is later than UWB. Subscript indicates turn radius.

	45°	90°	90°_{105}	90°_{185}	90°_{263}	135°	180°_{40}
Start	0.476	0.552	0.046	0.090	-0.012	0.572	0.146
End	-0.538	-0.729	-0.628	-0.454	-0.707	-0.322	-0.523

During movement, UWB is sampled four times faster than PDR. In most test cases, the user changes direction within one step, which introduces about one second of delay to register the final orientation. During this time, about four UWB updates already register the orientation change.

The increased positioning accuracy of the fusion approach is shown in Tab. II. The fusion of PDR and UWB improves the accuracy in both tracks with and without NLOS errors, yielding significantly more improvement when no NLOS is present. As expected, the introduction of NLOS leads to a decreased accuracy in both tracks. Fig. 5 shows the positioning of the PDR-EKF, the UWB-EKF and the fused position using PDR or UWB updates for a 90° turn with NLOS. The recording shows several interesting properties of the fusion. At the start, the UWB measurements show a varying bias in positive Y direction. This also leads to an initial bias for the PDR fusion. The variance in the Y direction is compensated to a degree by PDR. However, this means that the initial bias is upheld by the fusion with PDR. Overshooting of the UWB-EKF is visible at the turning point due to the delayed convergence to the new orientation. A slight overshoot of the fusion EKF is also visible right before the PDR update of the turn. This update sets the fused position on the ground truth. A bias of the PDR-EKF position used in this update of about 0.5 m in negative X direction is visible. Afterwards both UWB and PDR-EKF converge to the new true position. With an initial offset caused by orientation or positioning errors in the beginning, PDR gradually approaches recent measurements. However, an initial error means that the error state is prolonged by the fusion with PDR when UWB is already converging on the true position. This highlights the importance of a reliable initial position and orientation.

TABLE II: Average distance to ground truth for localization through fusion with PDR and for Kalman-filtered UWB alone in meters. With and without introduced NLOS errors while walking straight and turning by 90°.

	90°		Straight	
	w/ NLOS	w/o NLOS	w/ NLOS	w/o NLOS
Fusion	0.222	0.143	0.266	0.079
UWB	0.237	0.160	0.279	0.101
improvement % by fusion	6.3	10.6	4.7	21.8

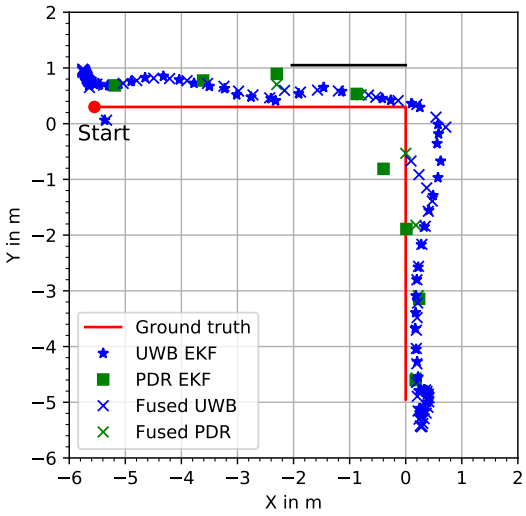

Figure 5: A right turn with NLOS. The object blocking UWB is shown as a black bar. Overshooting after the turn is reduced by PDR.

VIII. Conclusion

In this paper, we describe a localization framework using different kinds of localization sources. We propose a fusion architecture that distinguishes three types of positioning sources: absolute positioning, relative positioning on predefined axes, and relative positioning measuring velocity and heading change. The fusion is independent from the exact type of sensor and combines relative and absolute positioning to increase the overall accuracy and reliability. We show that PDR and UWB processed by an EKF exhibit complementary properties. UWB is affected by NLOS which is mitigated by fusion with PDR. Similarly, the PDR orientation drifts over time and lacks an absolute reference. Therefore, we use the orientation change together with the velocity vector of the fused location state. Our experiments verify the improvement of the fused positioning accuracy in comparison to UWB alone. However, an unreliable initial position and orientation leads to temporary worsening of accuracy by the relative position updates. The positioning accuracy will be tested in a real industrial environment in future works. Additionally, we plan to test the framework with other sensors.

Acknowledgements

This work has been achieved in the European ITEA project "OPTimised Industrial IoT and Distributed Control Platform for Manufacturing and Material Handling (OPTIMUM) and has been funded by the German Federal Ministry of Education and Research (BMBF) under reference number 01IS17027. We want to thank all partners in the OPTIMUM project for the stimulating discussions and their contributions to the project. All project partners can be found on https://itea3.org/project/optimum.html.

References

[1] B. Silva, Z. Pang, J. Akerberg, J. Neander, and G. Hancke, "Experimental study of UWB-based high precision localization for industrial applications," in *Proceedings of the 2014 IEEE International Conference on Ultra-Wideband*, Paris, France, 2014.

[2] J. F. Schmidt, D. Neuhold, J. Klaue, D. Schupke, and C. Bettstetter, "Experimental Study of UWB Connectivity in Industrial Environments," in *Proceedings of the 24th European Wireless Conference*, Catania, Italy, 2018.

[3] A. R. Jimenez Ruiz and F. Seco Granja, "Comparing Ubisense, BeSpoon, and DecaWave UWB Location Systems: Indoor Performance Analysis," *IEEE Transactions on Instrumentation and Measurement*, vol. 66, no. 8, pp. 2106–2117, 2017.

[4] R. Faragher and R. Harle, "An Analysis of the Accuracy of Bluetooth Low Energy for Indoor Positioning Applications," in *Proceedings of the 27th International Technical Meeting of The Satellite Division of the Institute of Navigation (ION GNSS+ 2014)*, Tampa, USA, 2014, pp. 201–210. [Online]. Available: http://www.ion.org/publications/abstract.cfm?jp=p&articleID=12411

[5] K. Lin, W. Wang, Y. Bi, M. Qiu, and M. Mehedi Hassan, "Human localization based on inertial sensors and fingerprints in the Industrial Internet of Things," *Computer Networks*, vol. 101, pp. 113–126, 2016.

[6] R. Harle, "A survey of indoor inertial positioning systems for pedestrians." *IEEE Communications Surveys and Tutorials*, vol. 15, no. 3, pp. 1281–1293, 2013.

[7] I. Skog, P. Handel, J.-O. Nilsson, and J. Rantakokko, "Zero-velocity detectionan algorithm evaluation," *IEEE Transactions on Biomedical Engineering*, vol. 57, no. 11, pp. 2657–2666, 2010.

[8] L. E. Díez, A. Bahillo, J. Otegui, and T. Otim, "Step length estimation methods based on inertial sensors: a review," *IEEE Sensors Journal*, vol. 18, no. 17, pp. 6908–6926, 2018.

[9] V. Pham, D. Nguyen, N. Dang, H. Pham, V. Tran, K. Sandrasegaran, and D.-T. Tran, "Highly accurate step counting at various walking states using low-cost inertial measurement unit support indoor positioning system," *Sensors*, vol. 18, no. 10, p. 3186, 2018.

[10] H.-h. Lee, S. Choi, and M.-j. Lee, "Step detection robust against the dynamics of smartphones," *Sensors*, vol. 15, no. 10, pp. 27 230–27 250, 2015.

[11] G. Rodríguez, F. Casado, R. Iglesias, C. Regueiro, and A. Nieto, "Robust step counting for inertial navigation with mobile phones," *Sensors*, vol. 18, no. 9, p. 3157, 2018.

[12] S. Vandermeeren, S. Van de Velde, H. Bruneel, and H. Steendam, "A feature ranking and selection algorithm for machine learning-based step counters," *IEEE Sensors Journal*, vol. 18, no. 8, pp. 3255–3265, 2018.

[13] A. Correa, M. Barcelo, A. Morell, and J. L. Vicario, "A review of pedestrian indoor positioning systems for mass market applications," *Sensors*, vol. 17, no. 8, p. 1927, 2017.

[14] F. Holzke, P. Danielis, F. Golatowski, and D. Timmermann, "A fusion approach for the localization of humans in factory environments," in *2018 IEEE Industrial Cyber-Physical Systems (ICPS)*. IEEE, 2018, pp. 59–64.

[15] F. Höflinger, R. Zhang, P. Fehrenbach, J. Bordoy, L. Reindl, and C. Schindelhauer, "Localization system based on handheld inertial sensors and uwb," in *Inertial Sensors and Systems (INERTIAL), 2017 IEEE International Symposium on*. IEEE, 2017, pp. 1–2.

[16] J. D. Hol, F. Dijkstra, H. Luinge, and T. B. Schon, "Tightly coupled uwb/imu pose estimation," in *Ultra-Wideband, 2009. ICUWB 2009. IEEE International Conference on*. IEEE, 2009, pp. 688–692.

[17] C.-I. Chesneau, M. Hillion, J.-F. Hullo, G. Thibault, and C. Prieur, "Improving magneto-inertial attitude and position estimation by means of a magnetic heading observer," in *2017 International Conference on Indoor Positioning and Indoor Navigation (IPIN)*. IEEE, 2017, pp. 1–8.

[18] S. O. Madgwick, A. J. Harrison, and R. Vaidyanathan, "Estimation of imu and marg orientation using a gradient descent algorithm," in *Rehabilitation Robotics (ICORR), 2011 IEEE International Conference on*. IEEE, 2011, pp. 1–7.

[19] R. Feliz Alonso, E. Zalama Casanova, and J. Gómez García-Bermejo, "Pedestrian tracking using inertial sensors," 2009.

[20] J. Lategahn, M. Müller, and C. Röhrig, "Robust Pedestrian Localization in Indoor Environments with an IMU Aided TDoA System," in *Proceedings of the 2014 International Conference on Indoor Positioning and Indoor Navigation (IPIN 2014)*, Busan, Korea, 2014.